2

Applied Optical Spectroscopy

Optical spectroscopy (a highly accountable reference on applied spectroscopy [1]), has for a long time been a basic tool for materials research and inspection. Optoelectronic innovations such as light sources, detectors, displays, etc. have their foundations in optical spectroscopy. There are different ways to specify optical spectroscopies such as transmission, reflection, fluorescence, spectroscopies. Quite often the spectral region defines the name of the spectroscopy such as UV, visible and NIR spectroscopy. The wavelength of electromagnetic radiation has a great role in the sense that it is sensitive to the basic units of the medium, namely electrons, atoms and molecules that experience the electromagnetic interaction. Nowadays, a rough way to separate different optical spectroscopies into two main classes is to speak of linear- and nonlinear optical spectroscopies. Well established protocols for the use of spectral devices, involving measurements in the field of linear optical spectroscopy, have been furnished, and spectrophotometers can be found in well-equipped laboratories, e.g., for medical and industrial inspection of samples, respectively. The number of industrial products or clinical samples that are inspected by spectral devices is very wide. One basic property is the colour of the sample.

Thanks to the cheaper optoelectronics, robust measurement systems have been built for routine inspection of solid, liquid, and gaseous samples. A variety of commercial miniature spectrometers with software for data processing and displaying are on the markets, and one can easily find up-to-date information of commercial spectrophotometers in the Internet. These miniature spectrophotometers are currently developed so that they offer relatively high resolution of wavelength and concentration of species for various types of real time measurements. Some of these spectrometers involve a fiber optic probe, for instance, for the detection of fluorescence from a product or monitoring fluorescent traces in turbid liquid media. The applications of optical spectroscopy are not limited to medical or industrial purposes only. Security of human beings is becoming more important with globalization. Therefore, spectrometers that can record lethal media such as bacteria and explosives have already been developed and are on their way to general use both in

civil and military environments. In forensic studies spectrometers are already everyday life. Future trend in realizing miniature spectrometers for process industry relies on micro electro mechanical systems (MEMS) produced by micro-lithography. Low price, durability and resistance against thermal and mechanical disturbances of such micro-spectrometers will enhance their application in hostile environments of process industry.

Nonlinear optical spectroscopy has been developing fast after the invention and development of high power lasers. Unfortunately, lasers and optical components for nonlinear optical spectroscopy have been relatively expensive, so far. Furthermore, due to complicated systems for materials inspection, and also weakness of the signal nonlinear optical spectroscopy, as far as we know, they have been able to evince great interest in the circles of process industry. One reason may also be that the theoretical background of nonlinear optical spectroscopy is rather difficult to understand for practioners, and may therefore hinder the adoption of such a technology, although it might solve many problems that appear, e.g., in adjusting process parameters. Fortunately, due to progress of powerful small size solid state lasers that can be purchased, nonlinear optical spectroscopy has a potential of becoming much stronger in the field of applied spectroscopy, especially biomedical optics.

In this chapter, we deal with typical optical spectroscopies that are currently used or are developed in the industry and research laboratories, and deal briefly the case of two-photon induced fluorescence that belongs to the field of nonlinear optics. We omit in this book the important sub-field of applied spectroscopy namely Fourier transform spectroscopy. There is a recent publication on this subject [2], which is highly recommended as a standard source for the physical backgrounds and applications of this sub-field. Here we just mention that Fourier transform infrared spectroscopy (FTIR) has various applications in analysis and identification of liquids, gases, and mixture of gases. Portable Fourier transform spectrometers have libraries in the memory of the computer that enable identification of different gas components. This has importance, in remote sensing of air pollution of exhaust from chimneys of factories and power plants, and also traffic. There are also military applications related to the FTIR technology.

2.1 Transmission Spectroscopy

Measurement of wavelength-dependent light transmission of a collimated light beam through transparent and colored planar solid objects is a routine procedure in materials inspection. Nowadays robust portable spectrophotometers for transmission measurement are commercially available. In many applications the spectrophotometer is assumed to monitor transmittance of a product. The transmittance is defined by the expression

$$T(\lambda) = \frac{I(\lambda)}{I_o(\lambda)}, \tag{2.1}$$

where I_o is the incident light intensity, I the transmitted light intensity upon the detecting area of the detector and λ the wavelength of the light. Using transmittance it is possible to gain information on the local thickness (d) of the product, which is assumed to be homogenous, via the Beer–Lambert law

$$I = I_o \exp(-\mu(\lambda)d), \tag{2.2}$$

where μ is a material parameter, i.e., the wavelength-dependent absorption coefficient of the medium. It is worth emphasizing that the absorption coefficient of a medium depends not only on the wavelength of the incident light but also on the thermodynamic condition of the sample. The temperature dependence of the object has to be specially taken into account in the measurement of a temperature sensitive sample. Typically there may appear fluctuation of the sample temperature, which is usually due to external heat sources, for instance, those present in industrial environments. Temperature-regulated spectrometers are recommended for such conditions. Thickness variation of a semitransparent sheet is obtained from (2.2). If we are working with a priori known material then the absorption coefficient has usually been measured in a laboratory at some appropriate spectral range. Hence, one can monitor the thickness change of a product using two or more different wavelengths, obtained by filtering from a white light source with a filter system, and using a two- or multidetector system. An alternative device may involve two or more lasers as collimated light sources, with well-known accurate wavelengths. Many times at industrial site external vibrations appear, for instance, due to the conveyor belt of the product. This means that the product, e.g., a plastic sheet may experience wavy or other type of motion. In order to get "a frozen" probed thickness, the probe beam is usually chopped. In the case of using two probing wavelengths they are usually chosen in a manner that the material absorbs at one wavelength say λ_1, whereas at λ_2 the absorption of the object is negligible. From (2.2) we can then solve the thickness of the object as follows:

$$d = \frac{1}{\mu(\lambda_1)} \ln \frac{I_o(\lambda_2)}{I(\lambda_1)}. \tag{2.3}$$

Detection of the intensity ratio by two detectors is of great importance since the aging of the light source is not a big issue then. If the product is a sheet that is moving on a conveyor belt and the sensing head has a fixed position, then thickness of the product along a line can be assessed. If a scanning measurement head is traversing across the machine direction, thickness of the products is obtained along a "Z-shaped" path. Obviously, one cannot probe the whole product with this kind of gauge, but usually this is not a big issue. Statistical analysis of the thickness and product history are usually stored into the memory of a computer so that properties of the product can be checked many years after its manufacture. In general, such storage of production history of any product is important. This is true particularly in the case of fracture of the purchased product because then it is usually possible to track production parameters of the broken product to check for responsibility of damage.

Transmission measurement by the two detector system is useful, not only in production environments of new products, but also in sorting of recycled plastic waste [3].

Basic metal industry that produces cold-rolled metal, which may take the form of a sheet or a roll, sells these products, for instance, to the automotive industry. Usually there is a requirement to protect the metal surface against corrosion, especially if the restoration time of the metal is relatively long. Thus from the customer side it is necessary to protect the metal sheet or a roll by a thin oil layer. It is important to optimize thickness of the oil layer since it has usually to be removed, before further processing, by using washing agents. For the sake of optimization of the thickness of the oil layer, it is measured at the metal production site; thickness of the layer can be checked by the customers also at their production sites. Optimization is important not only for proper protection against corrosion but also for reducing the amount of washing agents. The latter is of crucial importance for the purpose of decreasing pollution of the environments. The measurement technique may exploit, for instance, the absorption of the IR radiation in the protection oil, where absorbing units are hydrocarbons. Since the oil layer covers opaque metal, the measurement is based on transflectance, i.e., the oblique incident radiation is transmitted through the oil layer but reflected from the metal substrate. Analysis of the oil film thickness can be based on the utilization of (2.1). There are commercial portable devices available for monitoring oil film thickness. Reliability of the measurement result depends to some extent on the surface roughness of the metal product under the oil film. In Fig. 2.1 we show a principle of the oil film hand held measurement system of the transflectance on a spot of a metal roll.

Simultaneous measurement of film thicknesses and refractive indices of several solid layers is possible using the principles of inteference and reflection in thin films by scanning a spectrum from UV- to NIR region. The thickness, absorption and refractive index of a film on a substrate can be obtained using also an ellipsometer. Devices based on above mentioned principles are already in the markets.

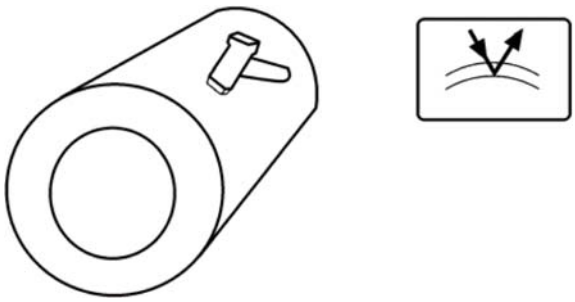

Fig. 2.1. Principle of oil film measurement using IR- absorption of hydrocarbon groups (*right*). An application is detection of oil surface density from steel sheet and roll (*left*)

Quite often we have to measure the transmission of liquids such as water where different constituents are mixed. In such a case we exploit a cuvette with well-known thickness such as 1 mm or 1 cm depending on the optical density of the sample. Then the transparency or colour of the liquid can be estimated with the aid of the transmission spectrum using the transmittance T. Real refractive index (n) and its change (Δn) are other quality parameters of the light absorbing liquid, which provide information about the concentration of the liquid. In the case of transmission measurement technique we can calculate, in addition to the absorption coefficient of the liquid, refractive index change as a function of the wavelength from measured data. From (2.2), one can solve the absorption coefficient, and then get the extinction coefficient (k) of the liquid, which is given by the expression

$$k(\lambda) = \frac{\mu(\lambda)\lambda}{4\pi}. \tag{2.4}$$

The real refractive index change and extinction coefficient are coupled together by Kramers–Kronig relations, and also by their modifications [4]. A useful method, especially when using band-limited transmission data only, is to extract the frequency-dependent real refractive index change from a so-called singly subtractive Kramers–Kronig (SSKK) relation [4], and thereafter perform a cross checking of the calculated data by the conjugated SSKK relation. The two SSKK relations require an anchor point where optical constant is a priori known. The information at the anchor point can usually be measured by other means, e.g., in the case of liquids, by a reflectometer. The SSKK relations are as follows:

$$n(\omega') - n(\omega_1) = \frac{2(\omega'^2 - \omega_1^2)}{\pi} P \int_0^\infty \frac{\omega k(\omega)}{(\omega^2 - \omega'^2)(\omega^2 - \omega_1^2)} \mathrm{d}\omega, \tag{2.5}$$

$$\frac{k(\omega')}{\omega'} - \frac{k(\omega_1)}{\omega_1} = \frac{2(\omega'^2 - \omega_1^2)}{\pi} P \int_0^\infty \frac{n(\omega) - n_\infty}{(\omega^2 - \omega'^2)(\omega^2 - \omega_1^2)} \mathrm{d}\omega, \tag{2.6}$$

where ω_1 is the anchor point frequency, P denotes Cauchy principal value and n_∞ is the high energy value of the refractive index. A code of a numerical algorithm for the SSKK analysis is presented in the book of Lucarini et al. [4].

For example in Fig. 2.2, we show the real refractive index change and extinction coefficient of 12 different commercial red wine products. First the transmittance of the red wine samples is measured using 1 mm cuvette at room temperature. The extinction coefficient is calculated with the aid of (2.4), and the refractive index change is calculated using (2.5). One application of the complex refractive index data is to help wine producers in research and development of red and other wines. Another application is to test the authenticity of purchased wine, in other words to check that the bottle and its etique match with the contents. This is to prevent counterfeit of wine and other drinks.

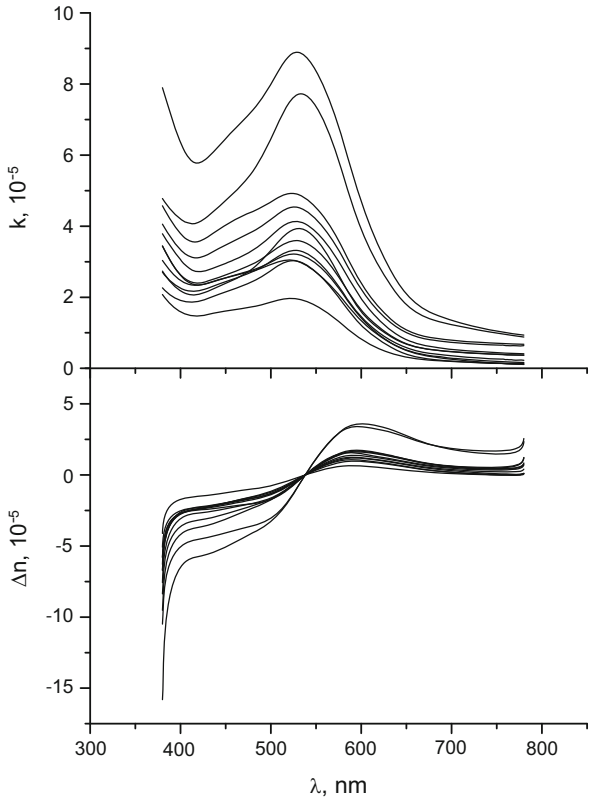

Fig. 2.2. Extinction coefficient (*upper panel*), and real refractive index change (*lower panel*) of some commercial red wines

In Fig. 2.2 one can identify the anthocyanins in the vicinity of 520 nm due to strong absorption of light. This is important in the color formation of red wines [5]. Color is considered as an important factor of red wine quality. Color coordinates (CIE Lab) of red wine can be calculated from the transmission spectrum. Another quality factor of red wine is the concentration of tannins which can be recognized due to strong light absorption at the vicinity of 280 nm.

Transmittance data of wine products can be utilized in quality inspection during and after the fermentation process. Fiber optic sensors provide means for in situ optical inspection of optical properties of wines [6]. Naturally, transmission data can be utilized in screening of whiskies and other colored alcohol drinks.

A spectral analysis reveals that the set of 12 red wines differ from each other. Hence studying spectral features and the color of the red wine one can gain information, e.g., about the authenticity of the wine. This is an important method in preventing counterfeiting of red wines and other liquid products.

The absolute value of the refractive index of red wine provides information about the density of the wine which depends on alcohol and sugar contents. Absolute value is obtained usually by a refractometer. We will describe the measurement of refractive index of liquids in Sect. 2.3.

Since red wines are more or less turbid liquids, scattering of light has also a role in the detection of true transmittance. By choosing a thin cuvette this light scattering can be satisfactory eliminated. Measurement of turbidity of wines and other light scattering liquids is one indicator of the quality of such liquids. In the next section we deal with the issue of turbidity in more detail.

2.2 Measurement of Turbidity of Liquids

The light scattering theory of Mie [7] is the basis of light interaction with spherical scattering centers, whose size matches the wavelength of the incident light, in gas or liquid phase. The theory of Mie works well in such situations where mono- or polydispersive spherical scatterers, with well known complex refractive index, occupy a relatively low volume fraction in the host medium. If the shape of the scatterer is complex, Mie theory becomes invalid. Furthermore, if the complex refractive indices of different types of scatterers, appearing simultaneously in the scattering volume of probe light is not known, one usually faces problems in rigorous interpretation of the measured signal. However, if we do not want to know specific properties of the scatterers but merely wish to gain information on the turbidity of the liquid, i.e., reduction of transparency of a liquid caused by undissolved matter, simple measurement geometry can be exploited. A modern device for the measurement of turbidity is called a nephelometer. The idea behind this device is to measure light scattering at 90° scattering geometry as shown in Fig. 2.3. Although the signal is a nonlinear function of turbidity, this geometry is sensitive to light scattering from particles.

The unit turbidity of this device is nephelometric turbidity unit (NTU) that may range between 0 and 10 000 NTU. Calibration is performed against

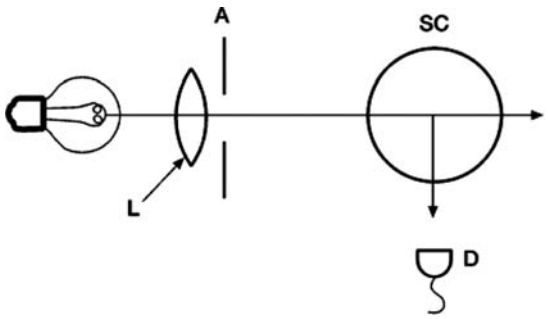

Fig. 2.3. Schematic diagram of a nephelometer. L, lens; A, aperture; SC, sample cell; and D, detector

formazin standard. It is obvious from Fig. 2.3 that the detection of scattered light depends not only on the concentration of the scatterers (multiplescattering) but also on the absorption of light by the scatterers and the liquid host, as well as on the spatial refractive index changes of the scattering medium. Evidently, it is difficult to derive a general theory for analysis of the signal. Thus we usually simply make use of the intensity of the light detected at the 90° scattering angle. Naturally, other scattering angles can be utilized in the assessment of turbidity in a wider scope as it has been shown for port wine [8] by recording turbidity of the port wine, during the production process, as a function of wavelength. Multifunction commercial sensors for monitoring quality of process waters in industry, or wastewater in treatment plants, are commercially available and include also the mode of gaining the turbidity. Process monitoring robust devices have been designed and produced, for measurement of consistency of pulp solutions in paper industry. The problem of the coloration of the turbid sample is usually avoided by choosing the operation wavelength at infrared region. In the event of strong turbidity, the backscattering measurement mode of the turbidity sensor is favorable. In the same measurement head forward- and backscattering measurement modes can be included in order to cover wide dynamical range of the turbidity. The common problem with an optical sensor head, when monitoring liquids of biological or industrial origin, is the contamination of the probe window. One solution to avoid this is to implement ultra sonic cleaning unit in the sensor head. Development of coating technology for noncontaminating surfaces is in strong progress, and the trend is to utilize nanostructures as over layers of the product, such as a wide variety of window materials.

In Table 2.1 we show NTU readings, in addition to the refractive index, of the 12 commercial red wines. Obviously, turbidity is subject to stronger fluctuation than the refractive index of these red wine samples.

Table 2.1. Production country, refractive index, alcohol volume % and turbidity of a set of 12 commercial red wine samples

Sample	Country	Refractive index (ABBE)	Alcohol %	Turbidity (NTU)
1	Italy	1.3440	12	5.6
2	Spain	1.3444	12.5	29
3	Spain	1.3441	12.5	24
4	France	1.3437	13	20
5	Chile	1.3462	14	190
6	France	1.3451	13	24
7	South Africa	1.3452	13.5	47
8	France	1.3451	12	10
9	Portugal	1.3439	12.5	54
10	USA	1.3448	13	43
11	France	1.3442	13.5	9.4
12	Argentina	1.3452	14	64

2.3 Reflection Spectroscopy

In this section we deal with the reflection measurement mode that has practical utility both in inspection of liquids and porous media. In the case of liquids a probe window can be introduced for on-line operation at industrial site in order to monitor the process parameters of the liquid condition. The measurement system may yield feedback to a process- or central computer for the purpose of optimizing and controlling the process parameters. In the case of porous media the inspection usually happens at the laboratory of the industrial site; depending on the object, on-line devices can also be furnished.

2.3.1 Refractometer

In the context of liquids, their refractive index is a basic optical quantity that is used in quality inspection. By measurement of the refractive index we can identify different liquids, get information on concentration of sugar, salt, proteins, acids, etc. diluted in water, alcohol in water, lactose in milk and so on. The principles of light reflection and refraction have found applications, especially, in inspection of refractive index of transparent liquids products and also process liquids of industrial processes. A classical refractometer is based on the Abbe refractometer. This device makes use of total reflection of light, as follows:

$$n = \sin\theta_{\mathrm{c}}, \tag{2.7}$$

Where n is the relative refractive index, i.e., the ratio $n = n_{\mathrm{liquid}}/n_{\mathrm{prism}}$ and θ_{c} is the critical angle of total reflection. The refractive index of the prism is a priori known. Hence by measurement of the critical angle, one gets the refractive index of the liquid. Dispersion data of typical prism materials can be found, for instance, from catalogues of companies that sell optical elements.

There are various types of commercial refractometers both for laboratory and industrial environments. Typically they measure refractive index of juice, beverages, soft drinks, wines and beer, and milk products in the food stuff industry. Naturally they have applications also in the fields of chemical, petrochemical and pharmaceutical industries. In the construction of a refractometer a LED or a white light source can be used as a light source. Using a filter some specific wavelength from a relatively wide spectral range light source, usually corresponding emission line of sodium in the vicinity of 589 nm, is chosen for monitoring of the real refractive index of the liquid to be inspected. It is possible to also use a laser as a light source of the refractometer. Aging of the light source is not a critical factor since the idea is to find the border of abrupt change of the intensity of the reflected light at the critical angle of incidence. The signal is detected by a linear photodiode array or a CCD-camera. In environments where the liquid is hot the sensor head is cooled by water circulation. For measurement of the refractive index of high pressure liquid the mechanical resistance of the sensor head is an issue. Wear of the probe window, in monitoring high pressure liquid flow, can be minimized by choosing

sapphire as the prism material. There are multihead configurations for in-line monitoring of process liquids in piping systems of process industries. Accuracy of the measurement of the refractive index is about 10^{-4}.

In the event of light absorbing and/or turbid liquids the concept of total reflection becomes questionable. Indeed, the classical Abbe device is based on the abrupt jump of the reflected light intensity at the critical angle of reflection. For instance, for colored liquids there is no such abrupt jump of the reflected light intensity for a fixed wavelength of the incident light. It means that we cannot locate the critical angle. This is a problem that can be overcome by recording the reflected light intensity as a function of the angle of light incidence, and forming the second derivative from the reflectance. The maximum of the derivative gives the location of the apparent critical angle. Color and turbidity of the liquid is no more a great issue in design and construction of modern process refractometers. The refractive index interval obtained by a process refractometer depends on the choice of the prism material and the focusing geometry of the light that is incident on the prism–liquid interface. For instance, one can construct a device where a focused laser beam provides an angle distribution for the measurement of relatively small changes of the refractive index of the liquid. From the Internet one can check rather easily the availability of commercial refractometers.

2.3.2 Reflectometer with Wavelength Scanning Mode

Estimate on complex refractive index of opaque media, such as slurries, at wide spectral range can be obtained using a reflectometer and relevant spectra analysis methods [9]. An alternative apparatus is an ellipsometer, which provides information on the complex refractive index of solid sample but usually for a relatively narrow spectral range. The principle of ellipsometry can be utilized for monitoring purposes in process industry, but then one usually makes use of a laser light source. Fig. 2.4 shows a multifunction reflectometer, which was developed for the purpose of process water analysis in pulp and paper mills. One can chose different measurement modes with this prism reflectometer. These include scanning of the angle of incidence or the wavelength. In addition, linear polarization, such as *s*- and *p*-polarizations of the incident light can be chosen.

The spectra analysis is most convenient by using the Fresnel's formulas for reflectance of *s*- or *p*-polarized light as follows:

$$R_s(\omega) = \left| \frac{\cos\theta - \sqrt{N^2(\omega) - \sin^2\theta}}{\cos\theta + \sqrt{N^2(\omega) - \sin^2\theta}} \right|^2 , \tag{2.8}$$

and

$$R_p(\omega) = \left| \frac{N^2(\omega)\cos\theta - \sqrt{N^2(\omega) - \sin^2\theta}}{N^2(\omega)\cos\theta + \sqrt{N^2(\omega) - \sin^2\theta}} \right|^2 , \tag{2.9}$$

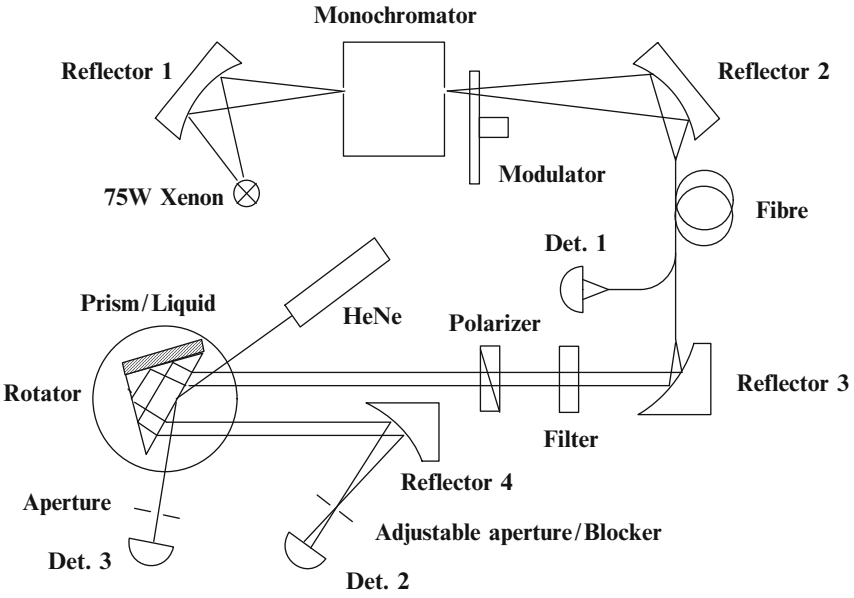

Fig. 2.4. Schematic diagram of a reflectometer

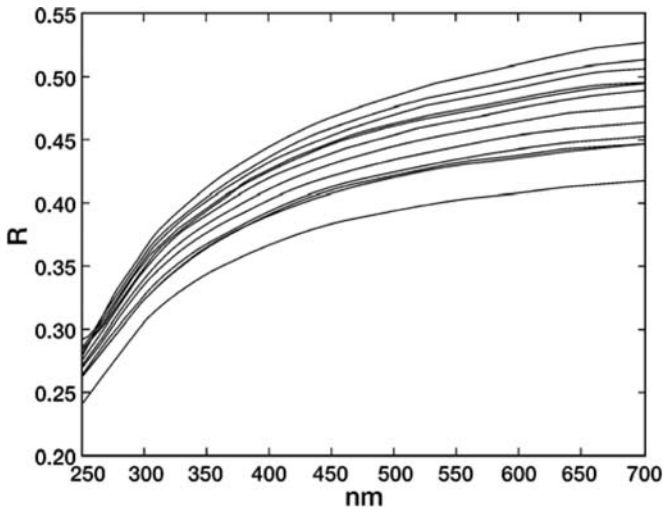

Fig. 2.5. Reflectance from 12 red wine samples as a function of wavelength. *Curves* were recorded by a reflectometer using s-polarized light

where θ is the angle of incidence, and N is the relative complex refractive index. The simplest case, in the frame of (2.8) and (2.9), occurs when the extinction coefficient of the liquid is so small that it can be neglected. In Fig. 2.5 we show reflectance for the 12 red wines that we have considered

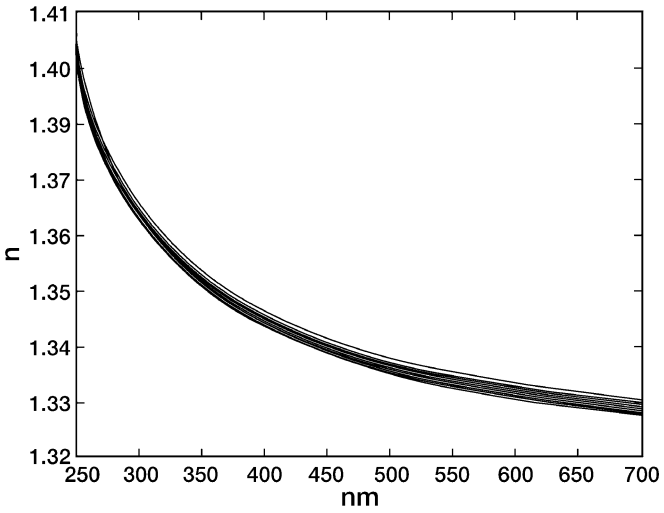

Fig. 2.6. Real refractive index of 12 red wines obtained using data of Fig. 2.5

previously. Data is recorded as a function of wavelength for a fixed angle of incidence and using s-polarized light. Under the assumption of relatively low extinction coefficient one can solve the refractive index of the red wines from (2.8), since there is only one unknown quantity namely the real refractive index n. Dispersion curves for the 12 red wines, using data of Fig. 2.5, are shown in Fig. 2.6. From Fig. 2.6 we observe that a relatively good way of monitoring concentration of the red wines can be found by integrating the refractive index curves. Use of the sodium D-line gives poorer sensitivity to some extent to distinguish differences between these wine samples.

In the case of scanning the angle of incidence for a fixed wavelength, an estimate of the complex refractive index can be obtained using an optimization method [9]. In this method one minimizes the least square sum of the difference between the reflectance obtained from the theory, (2.8) or (2.9), by inserting candidates for the complex refractive index N as follows:

$$S = \mathrm{Min} \sum_{\theta} \left[R_{\mathrm{m}}(\theta) - R_{\mathrm{t}}(\theta) \right]^2, \tag{2.10}$$

where R_{m} and R_{t} are the measured and theoretical reflectance, respectively.

Reflection coefficients of the medium,corresponding to the reflectance (2.8) and (2.9), are complex numbers due to the complex refractive index. Reflection coefficients for s- and p-polarized light can also be given in the following polar forms

$$\begin{aligned} r_s(\omega) &= |r_s(\omega)|\, \mathrm{e}^{\mathrm{i}\varphi_s(\omega)} \\ r_p(\omega) &= |r_p(\omega)|\, \mathrm{e}^{\mathrm{i}\varphi_p(\omega)} \end{aligned} \tag{2.11}$$

using the concepts of amplitude and phase of a complex number. In the wavelength scanning mode and fixed angle of incidence, an estimate of the spectral

dependence of the complex refractive index can be obtained by phase retrieval procedure using either singly or multiply subtractive Kramers–Kronig relations or by maximum entropy method (MEM) [4,10]. However, when utilizing SSKK one has to take care, especially when measuring reflection spectra, of the oblique incidence of p-polarized light [11]. In this particular case when the condition

$$n_\infty \leq \tan\ \theta \leq n_{\text{static}} \tag{2.12}$$

For a liquid (solids as well) is valid, K–K relations give an erroneous phase for the complex reflectivity. It means also that one gets erroneous complex refractive index of the liquid which can be solved using (2.9) and the latter form in (2.11). If the above condition (2.12) is not valid for p-polarized oblique incident light, or if one uses oblique incident s-polarized light, or the measurement happens at normal incidence then one can exploit the SSKK relations below, with one anchor point ω_1, for the phase retrieval and cross checking of calculated data

$$\ln|r(\omega')| - \ln|r(\omega_1)| = \frac{2(\omega'^2 - \omega_1^2)}{\pi} P \int_0^\infty \frac{\omega\phi(\omega)}{(\omega^2 - \omega'^2)(\omega^2 - \omega_1^2)} \mathrm{d}\omega, \tag{2.13}$$

and

$$\frac{\varphi(\omega)}{\omega'} - \frac{\varphi(\omega_1)}{\omega_1} = -\frac{2(\omega'^2 - \omega_1^2)}{\pi} P \int_0^\infty \frac{\ln|r(\omega)|}{(\omega^2 - \omega'^2)(\omega^2 - \omega_1^2)} \mathrm{d}\omega. \tag{2.14}$$

The reflectance and the reflection coefficient are coupled by the well-known relation $R = |r|^2$. Note that in practical analysis one has to limit the integration inside a finite spectral range. Such a procedure is a source of error. This error is reduced by the anchor point technique. The reason for the error decreasing is the better convergence of the SSKK relations than conventional Kramers–Kronig ones

Next we spend some time with phase retrieval using MEM, which may not be familiar for the readers. MEM can be used instead of K–K analysis for any situation, including the condition (2.12). Hence MEM is a more general method than K–K analysis, although the basis of MEM is not available in physics. MEM merely presents a mathematical method from information theory. Below we describe some features of MEM. In this method a reflectance spectrum, measured at a finite angular frequency range, is compressed into the interval between 0 and 1 by change of variable

$$\nu = \frac{\omega - \omega_{\text{start}}}{\omega_{\text{end}} - \omega_{\text{start}}}. \tag{2.15}$$

The complex reflection coefficient is obtained from a series expansion

$$r(\nu) \cong \frac{|d_o|\, \mathrm{e}^{\mathrm{i}\phi(\nu)}}{\left| \sum_{m=0}^{M} d_m \exp(-2\pi i m \nu) \right|}, \tag{2.16}$$

where the coefficients d_m are obtained from a set of Yule–Walker equations

$$\sum_{m=1}^{M} d_m C(m-p) = \begin{matrix} |d_o|^2, m = 0 \\ 0, m = 1, \ldots, M, \end{matrix} \tag{2.17}$$

and where autocorrelations C are obtained from the integral

$$C(\nu) = \int_0^1 |r(\nu)|^2 \exp\left[\mathrm{i}2\pi q\nu\right] \mathrm{d}\nu. \tag{2.18}$$

In the case of MEM we use data on the measured wavelength range only. That is to say no data extrapolations are performed. Since (2.16) is an approximation we usually have to correct the phase angle of the complex reflection coefficient. For that purpose we must have phase information at anchor points, which are located inside the measurement range. Usually two anchor points are enough to get a good estimate for the complex reflection coefficient, and therefore also for the complex refractive index of the medium, which is in liquid or solid phase. Angle correction is carried out using so-called "error phase" ϕ, which typically is a smooth nearly linear function with slow variation. The error phase can be presented as a polynomial interpolation

$$\phi(\nu) = \sum_{r=0}^{R} B_r \nu^r, \tag{2.19}$$

where the coefficients are obtained from a Vandermonde system

$$\begin{pmatrix} 1 & \nu_o & \cdot & \cdot & \nu_o^{\mathrm{L}} \\ 1 & \cdot & \cdot & \cdot & \nu_1^{\mathrm{L}} \\ \cdot & \cdot & & & \cdot \\ \cdot & & & \cdot & \\ 1 & \nu_{\mathrm{L}} & \cdot & \cdot & \nu_{\mathrm{L}}^{\mathrm{L}} \end{pmatrix} \begin{pmatrix} B_o \\ \cdot \\ \cdot \\ B_{\mathrm{L}} \end{pmatrix} = \begin{pmatrix} \phi(\nu_o) \\ \cdot \\ \cdot \\ \phi(\nu_{\mathrm{L}}) \end{pmatrix}. \tag{2.20}$$

In order to increase the linearity of the error phase another compression of the spectrum into a narrower spectral range is performed using the following data fitting procedure

$$|r_p(\nu)|^2 = \begin{matrix} |r(\nu)|^2, 0 \le \nu < w_K(\omega_1) \\ |r(\nu)|^2, w_K(\omega_1) \le \nu \le w_K(\omega_2) \\ |r(\nu)|^2, w_K(\omega_2) < \nu \le 1, \end{matrix} \tag{2.21}$$

where

$$w_K(\omega) = \frac{1}{2K+1}\left(\frac{\omega - \omega_1}{\omega_2 - \omega_1} + K\right), \tag{2.22}$$

and

$$\nu = \frac{w_K(\omega) - w_K(\omega_1)}{w_K(\omega_2) - w_K(\omega_1)}, \tag{2.23}$$

where K is a positive integer.

A crucial difference between K–K analysis and MEM is that in the case of the former we deal with logarithm of reflectivity, whereas with MEM we deal with the reflectivity itself. Hence, we can avoid the singularity which appears with logarithm as the complex abscissa is equal to zero.

In Fig. 2.7 we show reflectance and complex refractive index of a water–lignin solution, which is present in the process of pulping of wood for paper production. The water–lignin solution is optically very dense, which

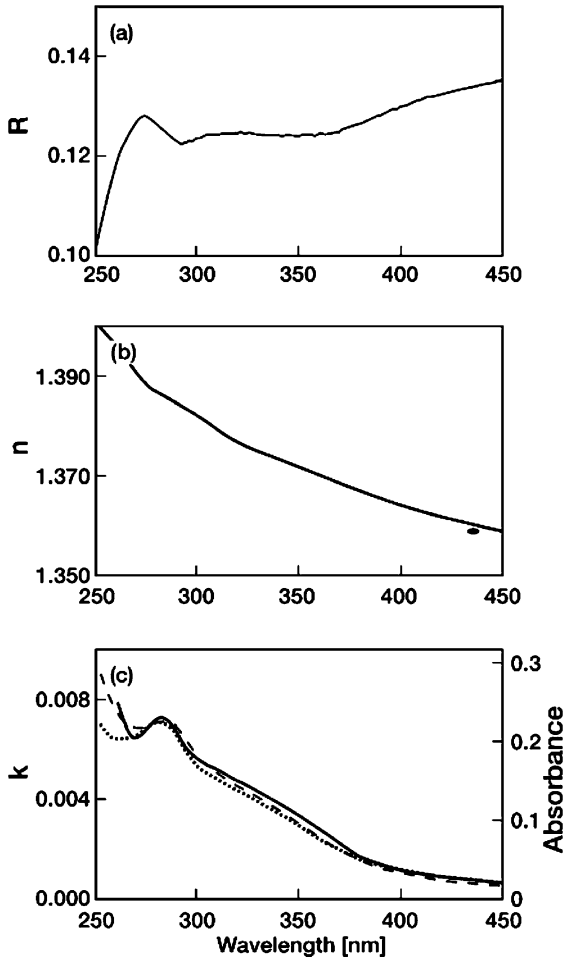

Fig. 2.7. (**a**) Reflectance, (**b**) real refractive index, and (**c**) extinction coefficient of a water–lignin solution

means that its intrinsic complex refractive index can be extracted only by measurement of the reflectance. The complex refractive index is extracted from the reflectance spectrum with the aid of the MEM analysis described above.

Due to scattering particles, which may be present in the liquid, the probe window of the prism is in many cases subject to contamination as a function of time. Sometimes it is possible to assess the correct reflectance by modeling the contamination as it was shown for pulping liquids [12, 13]. Fortunately the contamination layer can usually be removed by ultra sonic washing of the probe window.

After the somewhat lengthy theoretical treatment above we conclude this section by noting that the basic concept of the reflectometer (Fig. 2.4) provides a device for a multi-measurement scheme. It is possible to utilize a Dove prism that allows measurement of transmission, reflection and scattering of light from liquid samples with low or high turbidity. In addition rotation of light polarization can be used for measurement of optical activity of the liquid. With the reflectometer one gets information on the complex refractive index of extremely difficult objects such as offset inks used in printing houses [14, 15] and also birefringence of pigments used in paper industry [16]. Advantage with this kind of multifunction spectrometer is that one can avoid practical problems such as different practices, calibration, costs, maintenance, time consumption, and space requirements.

Surface Plasmon Resonance Spectrometer

Plasma oscillation in the surface mode can be generated using a prism, with one face coated by a thin metal film, and a laser as a light source. If the complex permittivities of the metal film and liquid sample are chosen properly, a surface plasmon resonance (SPR) can be exited for a fixed wavelength at an angle that is larger than the critical angle of reflection. SPR occurs when the wave number of the incident field parallel to the surface matches with the complex wave number of the surface plasmon. A detailed description of the physics of the SPR can be found from [17].

Typically the thickness of the metal film is ca. 50 nm. In laboratory experiments usually silver film is used due to the relatively strong SPR signal, whereas in commercial sensors gold film has been favored. Commercial SPR sensors make use of the Kretchmann's configuration [18] and a focused light beam impinging on the interface between the sample and the prism [19]. The focused beam automatically provides a range of incidence angles of the light rays; thus there is no need to rotate the probing prism. Obviously, the range of variation of the refractive index is limited by the magnitude of the cone of the incident light and the refractive index of the probe prism. However, usually the range of the variation of the refractive index (variation of concentration) of certain liquid can be estimated and taken into account in the construction of the SPR sensor. A photodetector, array of detectors or a CCD-camera is

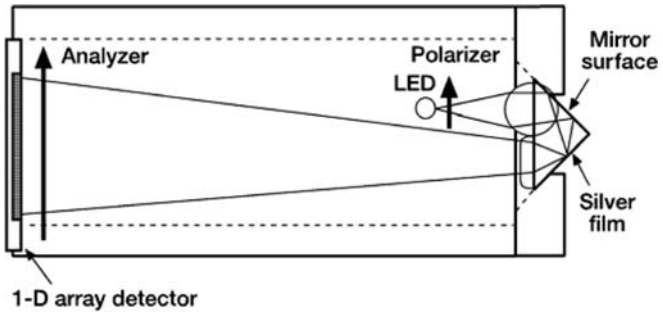

Fig. 2.8. Schematic diagram of SPR sensor

used for the detection of the spatial variation of a dip in the intensity of the reflected light. In Fig. 2.8 we show a schematic diagram of a SPR sensor.

The list of different kind of applications of a SPR sensor is long including, among others, measurement of optical properties and thickness of metal films, adsorption (or desorption) of gas molecules, drug discovery, food stuff applications, loadings of pigments used in paper, - paint and other sectors of industry, where liquids and pigments play important role. In some applications the metal surface has a special feature so that its texture is modified by introducing a lipid bi layer, adsorbed co-polymers, etc. This is important especially in monitoring of dynamic biological interactions where the liquid to be measured is under a flowing process in a flow cell that is coupled into the SPR measurement head [20]. Such a scheme is useful, e.g., in monitoring the kinetics of protein adsorption to biomaterials. A recent trend of SPR sensing is the research of proteins and protein interactions in low-gravity conditions on board a space station [21]. A DNA sensor based on SPR has been realized [22].

Most typical application of an SPR sensor is the measurement of the refractive index of a liquid. Analysis of refractive index of the sample is based on the following formula

$$\omega n_3 \sin\theta_{sp} = \sqrt{\frac{\varepsilon_1 \varepsilon_2}{\varepsilon_1 + \varepsilon_2}}. \tag{2.24}$$

This formula makes it possible to obtain at one wavelength of a laser, or at a discrete set of wavelengths, the refractive index of liquids by tuning the angle of incidence. Figure 2.9 illustrates reflectance dip curves for three homogenized milk samples. Sample 1 has 0.0004% fat, 3.48 proteins, and 4.96% lactose; sample 2 has 1.53% fat, 3.41 proteins, and 4.87% lactose; and sample 3 has 3.55% fat, 3.57 proteins and 4.74 lactose. All these samples contain water and small amounts of other constituents. After homogenization the size of fat particles is less than one micron and protein particles are even smaller. From Fig. 2.9 we can observe that location of minimum as well as half width of the dip are subject to change as a function of the fat volume percentage of the milk.

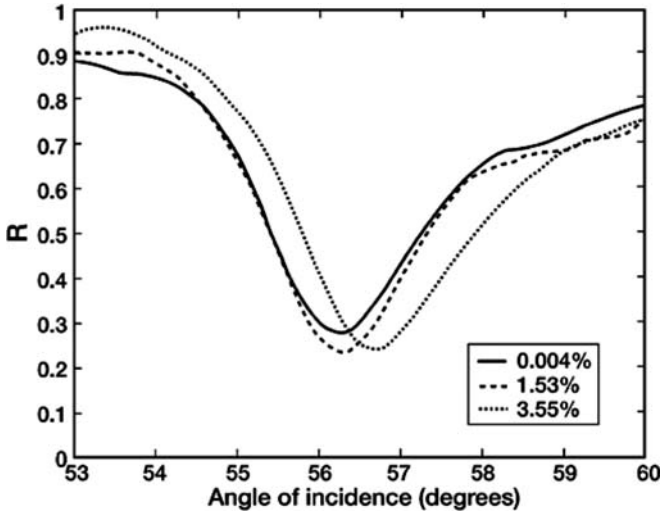

Fig. 2.9. SPR dips obtained for milk as a function of fat volume concentration [23]

Traditionally, the analysis of the reflectance curve in SPR sensing is based on observing resonance dip at the angle θ_{sp}, which shifts to different wavelengths due to the light dispersion of the liquid, metal film and the prism material. It is important that the system is thermally stable during the measurement since small temperature gradient may induce change location of the resonance angle.

In the case of surface plasmon resonance spectroscopy, we can make use of a reflectometer similar to that described in Sect. 2.3.2 but the face of the prism, which is in contact with the liquid, is covered by thin metallic film. Now the angle of incidence is fixed while the wavelength is scanned. While recording of the spectra, various finger prints of different species can be obtained. This is the major advantage of SPR spectroscopy, in addition to sensitivity to small variations in liquid concentration. In Fig. 2.10 are shown SPR dips that were obtained from water for different wavelengths. In the case of absorbing liquids ambiguity may appear in the location of the SPR dip and a single absorption peak [24].

Surface plasmons can be also generated from metallic particles embedded in a dielectric medium. Hence the interaction of the light waves does not depend on the use of a prism as coupler. Quite recently, research on nanostructures has become one of the most important fields in technology and life sciences. One of the most important fields is nanomedicine where new generations of cancer diagnostic and therapeutic means, which will dramatically improve cancer outcomes, are developed with aid of nanotechnology. In other words nanoparticles, such as gold nanoshells, quantum dots, etc. will be used for tissue targeting, sensing and imaging, and also localized therapy. An

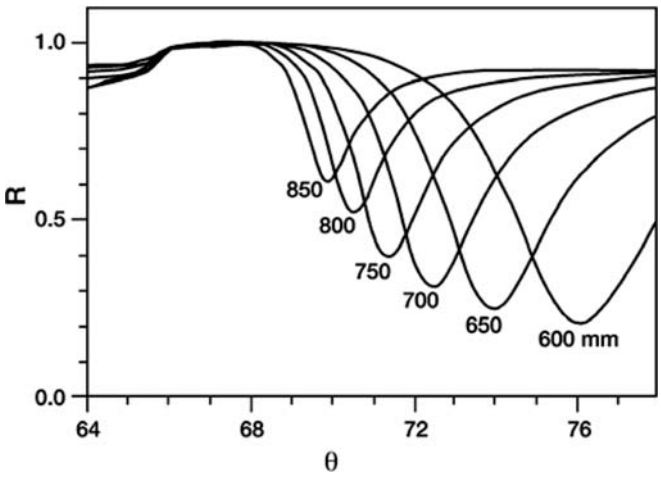

Fig. 2.10. SPR dips for water at different wavelengths. Step at the *curves* in the vicinity of 65° is due to the total reflection

advantage of nanoparticles is the use of lower doses. Gold nanospheres coupled to DNA or protein probes can be used in diagnostics of small amounts of proteins that appear in the case of cancer, cardiovascular disease, Alzheimer disease, etc. The unique property of a gold nanosphere is that one can probe proteins through optical phenomena. Quantum dots are usually nanoscale semiconductors with fluorescing tags. They absorb light at narrow spectral band but emit at long wavelengths at the infrared range. Quantum dots with protein coating can penetrate cells because cells regard them as proteins. Common aspect with nanoparticles is that their optical properties depend on their size, shape, and environment. Localized surface plasmon resonance spectroscopy in medical diagnostics that is based on the use of nanosensors is in progress [25]. In the event of using a large number of nanoparticles in medicine nanotoxicology may be an issue.

The case of several absorption peaks of dielectric nanoparticles, which are in a water matrix, appear simultaneously with the SPR dip was analyzed by Vartiainen et al. [26] from the reflectance data with the aid of the MEM. The extraction of the complex refractive index from SPR data is possible from the equations that are obtained by considering multiple Fresnel reflection in a thin film sandwiched between two media (liquid and prism) and with different complex refractive indices, respectively. The machinery for such an analysis is based on the reflectance

$$R_p(\theta) = \left| \frac{r_{\mathrm{pm}}(\theta) + r_{\mathrm{ml}}(\theta) \exp\left[2iA_z(\theta)d\right]}{1 + r_{\mathrm{pm}}(\theta) r_{\mathrm{ml}}(\theta) \exp\left[2iA_z(\theta)d\right]} \right|^2 , \tag{2.25}$$

where r_{pm} is the complex reflection coefficient for the prism–metal interface, r_{ml} is the reflection coefficient at the metal film–liquid interface, d is the

thickness of the metal film and A_z is the scalar component of the wave vector in the direction of the normal of the metal film. Furthermore,

$$r_{\mathrm{pm}} = \frac{\dfrac{A_{z,\mathrm{prism}}}{\varepsilon_{\mathrm{prism,r}}} - \dfrac{A_{\mathrm{zm}}}{\varepsilon_{\mathrm{mr}}}}{\dfrac{A_{z,\mathrm{prism}}}{\varepsilon_{\mathrm{prism,r}}} + \dfrac{A_{\mathrm{zm}}}{\varepsilon_{\mathrm{mr}}}}, \tag{2.26}$$

$$r_{\mathrm{ml}} = \frac{\dfrac{A_{\mathrm{zm}}}{\varepsilon_{\mathrm{mr}}} - \dfrac{A_{z,\mathrm{liq}}}{\varepsilon_{\mathrm{liq,r}}}}{\dfrac{A_{\mathrm{zm}}}{\varepsilon_{\mathrm{mr}}} + \dfrac{A_{z,\mathrm{liq}}}{\varepsilon_{\mathrm{liq,r}}}}, \tag{2.27}$$

where $\varepsilon_{\mathrm{prism,\ r}}$ is the relative permittivity of the prism, $\varepsilon_{\mathrm{mr}}$ the relative complex permittivity of the metal film (usually the bulk permittivity is used in data analysis) and $\varepsilon_{\mathrm{liq,r}}$ the corresponding relative permittivity of the liquid (or gas). The wave number is given by the expression

$$A_{zj} = \left[\varepsilon_{jr}\left(\frac{\omega}{c}\right)^2 - A_x^2\right]^{1/2}, \tag{2.28}$$

where

$$A_x = n_{\mathrm{prism}}\frac{\omega}{c}\sin\ \theta. \tag{2.29}$$

Before closing this section we emphasize that SPR data can also be exploited in the detection of thickness of the metal film on the prism face. This is important not only in basic research but applications where thickness of the metal film is subject to wear. For instance, wear can be due to laminar or turbid flow of solid particles that pass the probe window, or due to chemical corrosion. Monitoring of the metal film allows better calibration of the SPR gauge.

2.4 Measurement of Diffuse Reflection from Porous Media

Light interaction with porous media is complicated. Complications originate from multiple scattering of light (Mie scattering theory is invalid), random location, and different geometries and complex refractive indices of the particles that constitute the porous media. A simple example of such a porous medium is paper. Paper has a fiber network, fillers, fines, and pigments. Due to porosity of a medium, diffuse transmission and/or reflection of light appear. The diffuse light provides spectral data of the sample. One can use a photogoniometer for detection of the scattered light but such a device is tedious to use and rather expensive. Normally diffuse light is detected using a spectrophotometer, which includes an integrating sphere. The angle of light incidence is usually fixed near the normal incidence. It is possible to also measure specular

component of light with the integrating sphere. Portable spectrophotometers with white light sources incorporated by an integrating sphere are available, and such spectrophotometers can also be utilized for detection of the colour of the object.

In the event of thick samples, it is reasonable to use the diffuse reflection measurement mode. Examples of thick and light diffusing objects are, pharmaceutical tablets, pile of papers, ceramics and so on, which can be inspected using the diffuse light. Here we concentrate on the inspection of paper in some depth. Opacity is a crucial parameter of paper, especially for paper grades that are produced for printing purpose. Thus opacity is important in characterizing the quality of news papers, magazines, and books. High opacity means that one cannot distinguish printing on the opposite side of the paper. Obviously, high opacity (=high nontransparency) is a measure of the quality of paper for prints.Opacity depends on the thickness, refractive index of pigments and brightness of the paper. Brightness of paper in turn can be increased using whitening agents. In the laboratories of paper mills routine opacity measurements are taken from the products. ISO standard of opacity of paper is based on incident diffuse light which is recommended to be detected at zero angle ($D/0^\circ$). ISO opacity is defined as the reflectance ratio

$$\mathrm{OP} = \frac{R_o}{R_\infty}, \tag{2.30}$$

where R_o is the reflectance detected from a single paper sheet (background black) and R_∞ is the reflectance detected from a stack of paper sheets. Human vision, i.e., the response curve of the eye, is important for the appearance of opacity of paper.

A model devised by Kubelka and Munk (K–M) [27] has been used for the description of opacity of paper and other porous media. Detailed description of the K–M model and derivation of their formula can be found from [28]. In the K–M formula the ratio of absorption and scattering coefficients, K/S, is coupled with R_∞ as follows:

$$\frac{K}{S} = \frac{(1 - R_\infty)^2}{2R_\infty}. \tag{2.31}$$

Equation (2.31) is the basis, e.g., in optical measurement of moisture of paper. Moisture detection is based on the use of water peaks in the infrared spectral region. In the event of fluorescent porous objects, care has to be taken in the interpretation of diffuse spectra. In Fig. 2.11 we show diffuse reflection spectra gained from two different papers obtained from paper mill. It is evident from Fig. 2.10 that different paper grades cause different spectral features in paper. Such data is valuable, e.g., in research and development of paper products.

Figure 2.12 presents a modern multimode laboratory device for paper mills. There are various mechanical and optical measurement modes in the sensor head of Fig. 2.12, among others, the opacity of the paper.

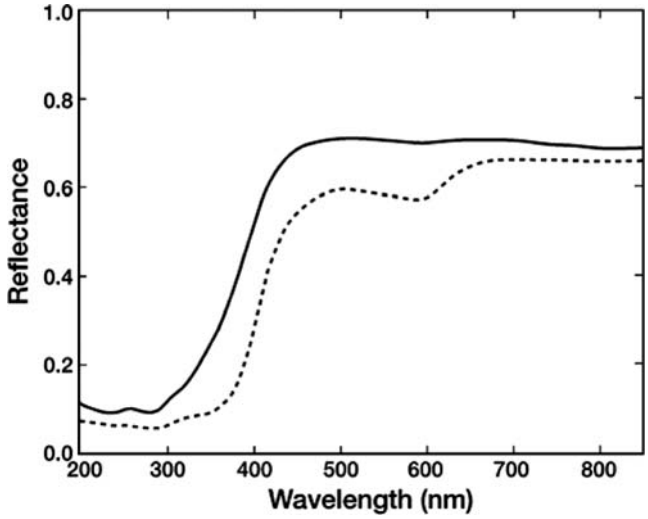

Fig. 2.11. Diffuse reflection from two different paper grades

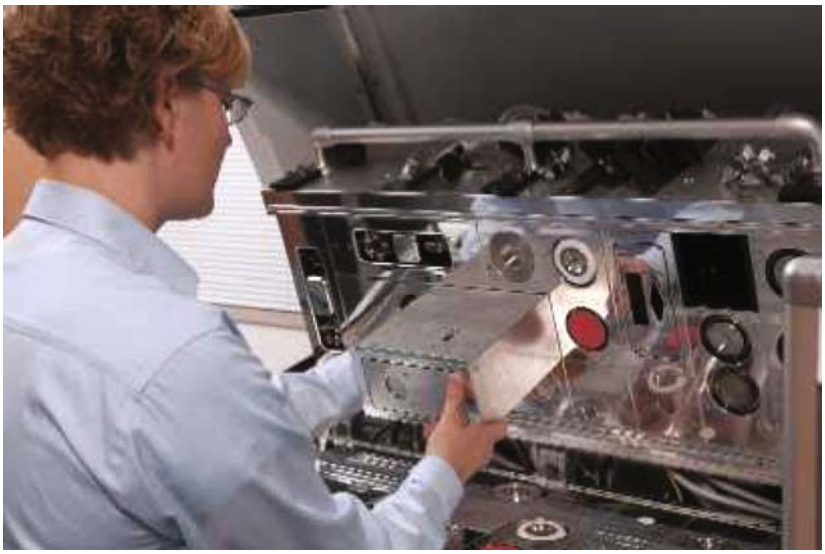

Fig. 2.12. Measurement head of PaperLab multifunction device for paper quality (Photo courtesy of MetsoAutomation)

2.5 On Estimation of Optical Constants of Porous Media

The overwhelming problem with porous media such as paper is usually the multiple scattering of light. Simple models for light scattering are usually insufficient for rigorous description of the interaction of light with porous

media. Yet, there is a desire to gain information also on the optical constants of such media. In the event that the pores or inclusions in a host media are so small that light scattering is negligible, one may try to utilize effective medium theory for the assessment of the optical constants, such as the effective complex refractive index, of the medium. Information on the effective complex refractive index can be obtained via measurement of reflectance and transmittance. A classical model that is often utilized is based on the effective medium theory devised by Bruggeman [29]. In this model one has to know a priori the volume fraction of the pores in the matrix; the diameter of the pore is disregarded. The model is suited best for the analysis of optical data of nanostructured media. In the case of spherical pores in two-component medium, the effective complex permittivity of the Bruggeman media is as follows:

$$f_h \frac{\varepsilon_h(\omega) - \varepsilon_{e\mathrm{ff}}(\omega)}{\varepsilon_h(\omega) + 2\varepsilon_{e\mathrm{ff}}(\omega)} + f_i \frac{\varepsilon_i(\omega) - \varepsilon_{e\mathrm{ff}}(\omega)}{\varepsilon_i(\omega) + 2\varepsilon_{e\mathrm{ff}}(\omega)} = 0, \tag{2.32}$$

where ε_h and ε_i are the complex permittivities of the two components, respectively. The volume fractions of the two components fulfil the relation $f_h + f_i = 1$. If the shape of the pore is different from a sphere, (2.32) can be generalized as follows [30]:

$$f_h \frac{\varepsilon_h - \varepsilon_{\mathrm{eff}}}{\varepsilon_{\mathrm{eff}} + g(\varepsilon_h - \varepsilon_{\mathrm{eff}})} + f_i \frac{\varepsilon_i - \varepsilon_{\mathrm{eff}}}{\varepsilon_{\mathrm{eff}} + g(\varepsilon_i - \varepsilon_{\mathrm{eff}})} = 0. \tag{2.33}$$

where factor g is a shape factor, which is equal to 1/3 for spherical pores. Effective permittivity can be solved from (2.33) as

$$\varepsilon_{\mathrm{eff}} = \frac{-h + \sqrt{h^2 + 4g(1-g)\varepsilon_i\varepsilon_h}}{4(1-g)}, \tag{2.34}$$

where

$$h = (g - f_i)\varepsilon_{_i} + (g - f_h)\varepsilon_h. \tag{2.35}$$

The concept can be generalized to hold for multiphase systems and anisotropic media. Unfortunately the effective medium model of Bruggeman is not valid for a great variety of porous products where the simple, different effective medium models cannot be applied. However, there is another approximate model that makes it possible to assess effective optical constants of light scattering media. It is based on the Wiener bounds [9] for a multiphase system which is as follows:

$$\begin{aligned} \frac{1}{\sum\limits_{j=1}^{J} \frac{f_j}{\varepsilon_j}} &\le \varepsilon_{\mathrm{eff}}, \\ \varepsilon_{\mathrm{eff}} &\le \sum_{j=1} f_j \varepsilon_j, \end{aligned} \tag{2.36}$$

where the permittivity ε_j may be a complex number. Since fill fractions fulfill the condition $\sum_j f_j = 1$, the f_js forms a barycentric coordinate system, which is useful in the estimation of effective permittivity of multicomponent composites [31].

The point of the Wiener bounds is that essentially the medium is considered as two extreme cases namely capacitors having parallel dielectrics or dielectrics in series. Such a treatment may yield rather tight upper and lower bounds for the wave-length dependent effective refractive index of media, and the inclusion itself. This was demonstrated in assessing the refractive index of concentric spherical shell of a copolymer, which is a plastic pigment for paint- and paper industry [32], and for assessment of optical properties of nanoparticles for nanomedicine [33].

2.6 Nonlinear Optical Spectroscopy

In the case of linear optical spectroscopy, the intensity of the probe light is so weak that optical properties of the medium do not change as a function of the amplitude of the light field. However, if we use high intensity lasers as light sources then there may appear observable dependence of the optical properties of the medium on light intensity. Thus, we may utilize such lasers for the study of nonlinear optical properties of media. This possibility opens a relatively wide window to gain various kinds of information on the medium to be inspected because the number of different kinds of nonlinear processes is rather high. We recommend readers interested in nonlinear optical processes to consult the text books of Shen [34] and Boyd [35]. Tunable lasers, where both intensity and wavelength of the radiation can be tuned, offer us means to gain nonlinear optical spectra. Nowadays, femtosecond lasers are popular for experiments in the field of time-resolved spectroscopy. Unfortunately, in most cases the lasers are expensive and experimental setups complicated to measure nonlinear optical spectra. Therefore, it may take time before these devices become popular for routine material analysis in industrial environments. Nevertheless, there is continuous progress towards valuable diagnostic devices in the field of life sciences. Microscopy, which makes use of nonlinear light interaction with biological samples, has been developed. Here we deal only with the case of fluorescence that is generated by two-photon absorption.

The interaction of weak or strong electric field with media can be described with the aid of the susceptibility (χ) of the medium. This susceptibility, which is related to the microscopic properties of the medium, comes from two contributions namely the linear susceptibility (χ_{L}) and nonlinear susceptibility (χ_{NL}). The former is always present, and it is closely connected to the complex refractive index of the medium. Information on the latter can be obtained in the presence of strong electric field only. According to the nonlinear processes, the nonlinear susceptibility has sub-divisions such as second-order ($\chi^{(2)}$),

third-order($\chi^{(3)}$), ..., multiple-order susceptibility ($\chi^{(n)}$). The strength of the interaction is described with the aid of polarization (P) of electric charges, typically electrons, as follows:

$$P = \chi^{(1)}E + \chi^{(2)}E^2 + \chi^{(3)}E^3 + \ldots, \tag{2.37}$$

where E is the amplitude of the electric field. Second-order processes appear only for media where the inversion symmetry of the potential function of the electrons is broken. An important application of the second-order susceptibility is the surface analysis on an interface between two different media. Third-order processes appear with all materials, i.e., those having either isotropic or anisotropic structure.

Two-photon absorption is governed bythe third-order nonlinear susceptibility of the medium and in this case the Beer–Lambert absorption law has to be modified as follows [9]:

$$I = \frac{\frac{\mu}{\gamma}}{\left(1 + \frac{\mu}{\gamma I_o}\right) e^{\mu d} - 1}, \tag{2.38}$$

where μ is the linear absorption coefficient, and γ is the absorption coefficient of two-photon absorption, which depends on the wavelength of light. The energy diagram of two-photon excitation and emission is illustrated in Fig. 2.13. The point is the simultaneous absorption of two photons at the same place.

By focusing laser radiation, obtained from a solid state laser, one can choose the volume inside the medium where the nonlinear two-photon absorption occurs. This technique has the advantage that the absorption of the laser line is negligible. In a chromophore two-photon, excitation may induce fluorescence. Thus it is possible to perform, for instance, bioaffinity assaying

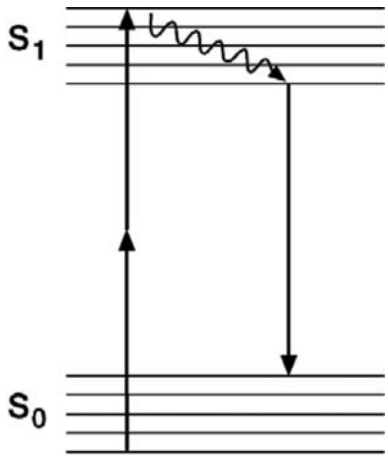

Fig. 2.13. Two-photon excitation and emission

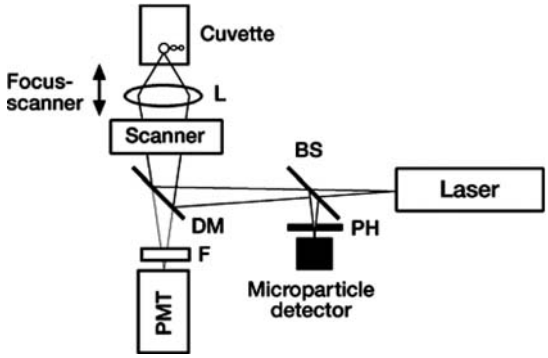

Fig. 2.14. Bioaffinity assaying using two-photon fluorescence. BS, beam splitter; PH, pinhole; D, dichroic mirror; F, filter; and PMT, photomultiplier

with the aid of the two-photon excitation [36]. Such a device is believed to have applications in drug discovery and clinical tests at hospital laboratories. One advantage of this apparatus is that time-consuming preparation of blood samples is not necessary. In Fig. 2.14 we show a schematic diagram of the two-photon fluorescence apparatus [36], which can be used in cytometric studies for detection of particles in turbid matrix.

Before closing this section we remark that conventional fluorescence, i.e., light emission from chromophores at wavelength that is higher than the excitation wavelength, has been utilized both in engineering and life science for the detection of organic media. Commercial devices based on fluorescence have been developing strongly in the field of drug discovery. The key word in drugs discovery is the high-throughput.

2.7 Conclusions

Optical spectroscopy is a well-established technique. Nevertheless, there is a strong development of small size and inexpensive spectrometers for materials inspection both in industry and life sciences. There will be great challenges ahead with optical spectroscopy, especially in monitoring of pollution of the environment caused by industry and the society. We believe that optical spectroscopy will provide at least a partial solution for monitoring the condition of the environment. One can easily understand that due to climate change, the quality of air, drinking water and water bodies such as lakes, rivers and coastal waters is already a big issue. Sensors based on optical spectroscopy are already on markets for on-line monitoring of water quality. A future trend will be that robust optical sensors, using spectra analysis, can be located in remote places, while on-line data and power consumption of the sensor is realized either using a solar cell or wind power or both. These sensors provide real time wireless information on water quality using technology related to

cellular phones. Early warnings reach the cellular phone of relevant persons, and in case of emergency a text message to these phones can reach all persons who may suffer contaminated water.

In future the development of small size spectrometers kind of micro machines which can be send, for example with industrial process water for sensing purpose, and which sensor may vanish once the duty cycle is over, will improve real time process monitoring. In the case of a closed water cycle, which would reduce the current use of huge amount of water in some industrial processes, role of reliable sensors for water quality inspection will be very crucial.

http://www.springer.com/978-3-540-71926-7

Optical Measurement Techniques
Innovations for Industry and the Life Sciences
Peiponen, K.-E.; Myllylä, R.; Priezzhev, A.V.
2009, VIII, 158 p., Hardcover
ISBN: 978-3-540-71926-7